

# Thermodynamic and magnetic properties of the layered triangular magnet $\text{NaNiO}_2$

P. J. Baker,<sup>1</sup> T. Lancaster,<sup>1</sup> S. J. Blundell,<sup>1</sup> M. L. Brooks,<sup>1</sup> W. Hayes,<sup>1</sup> D. Prabhakaran,<sup>1</sup> and F. L. Pratt<sup>2</sup>

<sup>1</sup>*Clarendon Laboratory, University of Oxford, Parks Road, Oxford OX1 3PU, United Kingdom*

<sup>2</sup>*ISIS Muon Facility, ISIS, Chilton, Oxon. OX11 0QX, United Kingdom*

(Dated: May 1, 2019)

We report muon-spin rotation, heat capacity, magnetization, and ac magnetic susceptibility measurements of the magnetic properties of the layered spin-1/2 antiferromagnet  $\text{NaNiO}_2$ . These show the onset of long-range magnetic order below  $T_N = 19.5$  K. Rapid muon depolarization, persisting from  $T_N$  to about 5 K above  $T_N$ , is consistent with the presence of short-range magnetic order. The temperature and frequency dependence of the ac susceptibility suggests that magnetic clusters persist above 25 K and that their volume fraction decreases with increasing temperature. A frequency dependent peak in the ac magnetic susceptibility at  $T_{sf} = 3$  K is observed, consistent with a slowing of spin fluctuations at this temperature. A partial magnetic phase diagram is deduced.

PACS numbers: 76.75.+i, 75.50.Ee, 75.30.Gw

Geometrically frustrated transition metal oxides exhibit a rich variety of magnetic behavior due to competing interactions. A significant degeneracy in the ground state leads to such phenomena as spin glass<sup>1</sup>, spin liquid<sup>2</sup>, and spin ice<sup>3</sup> phases. Triangular lattice antiferromagnets exhibit a variety of these phenomena<sup>4</sup>. When the triangles forming the lattice are distorted from equilateral to isosceles there is a partial release of the geometrical frustration, which can lead to more unusual forms of magnetic order<sup>5,6,7</sup>. Among triangular lattice antiferromagnets,  $\text{LiNiO}_2$ <sup>8</sup>,  $\text{AgNiO}_2$ <sup>9</sup>, and  $\text{NaNiO}_2$  have somewhat enigmatic magnetic behavior. The difficulty of producing stoichiometric  $\text{LiNiO}_2$  has led to a variety of sample-dependent results<sup>10</sup>.  $\text{AgNiO}_2$  can be produced in stoichiometric form but no magnetic Bragg peaks have so far been reported<sup>9</sup>. Recently neutron powder diffraction studies have determined the low temperature magnetic structure of  $\text{NaNiO}_2$ <sup>11,12</sup>. Darie et al.<sup>11</sup> find the ordering of the magnetic moments at 4 K to be a slight modification of the A-type antiferromagnetic ordering previously proposed<sup>13</sup>. The magnetic moments were found to be aligned at an angle of  $100(2)^\circ$  to the  $a$ -axis in the  $ac$  plane with no moment along the  $b$ -axis. A peak in the magnetic susceptibility interpreted as the Néel temperature,  $T_N$ , has been observed around 20 K<sup>13,14,15</sup>. The Curie-Weiss constant,  $\theta_{CW} = +36$  K<sup>15</sup>, shows the presence of ferromagnetic interactions above  $T_N$ .

The intralayer and interlayer exchange constants of  $\text{NaNiO}_2$ ,  $J_{\parallel} = -13.3$  K and  $J_{\perp} = 1.3$  K, were determined from a model assuming an A-type antiferromagnetic ordering with an anisotropy field<sup>16</sup>; the layers are sufficiently strongly coupled to permit long range magnetic order below  $T_N$ . The Ni-O-Ni bond angles are  $\approx 95^\circ$  at room temperature<sup>17</sup>. An undistorted  $90^\circ$  geometry favours weak ferromagnetic superexchange, while a large deviation from a  $90^\circ$  bond angle can reverse the sign of this exchange coupling<sup>18</sup>. In  $\text{NaNiO}_2$  it appears that despite the distortion, in-plane ferromagnetic coupling prevails, though the precise nature of the spin and orbital ordering remains under discussion<sup>19,20,21</sup>.

Above 480 K the space group of  $\text{NaNiO}_2$  is rhombohe-

dral ( $R\bar{3}m$ ) and there is a cooperative Jahn-Teller transition to a low temperature monoclinic ( $C2/m$ ) phase below this temperature<sup>17</sup>. The low-temperature structure can be considered to be layers of  $\text{NiO}_6$  octahedra in the  $ab$  plane, with a trigonal distortion lengthening the Ni-O bonds in the  $ac$  plane along an axis at  $41^\circ$  to the  $c$ -axis of the crystal. The  $\text{Ni}^{3+}$  ( $3d^7$ ) ion is in the low spin state ( $t_{2g}^6 e_g^1$ ,  $S = 1/2$ ), so the ground state is a singly-occupied  $|3z^2 - r^2\rangle$  orbital with  $z$  along the axis of the Jahn-Teller induced trigonal distortion<sup>17</sup>.

In this paper we present the results of zero-field muon spin rotation ( $\mu\text{SR}$ ) experiments<sup>22</sup> on polycrystalline  $\text{NaNiO}_2$  together with heat capacity and magnetic susceptibility measurements. These provide evidence of long range magnetic order below  $T_N$ , a slowing of spin fluctuations at low temperature, and short range magnetic order within a small temperature region above  $T_N$ , with magnetic correlations persisting to higher temperature.

$\text{NaNiO}_2$  was prepared from  $\text{Na}_2\text{O}_2$  and  $\text{NiO}$  powders heated at  $700^\circ\text{C}$  for 100 hours under pure oxygen flow, with intermediate grinding. X-ray powder diffraction showed that the impurity concentration was below the 2% resolution limit of the apparatus. Heat capacity data measured in magnetic fields between 0 and 14 T, taken with a Quantum Design PPMS, are shown in Fig. 1(a). In zero field the transition at  $T_N = 19.5$  K is seen as a rather broad peak, and there is no evidence for other phase transitions below 30 K. With increasing magnetic field the temperature of this peak decreases to about 14 K (see Fig. 1(a)).

Magnetic susceptibility data, taken using a Quantum Design MPMS SQUID magnetometer are shown in Fig. 1(b), (d) and (e). The high temperature dc susceptibility data, shown in Fig. 1(e), are consistent with  $\theta_{CW} = +36$  K<sup>15</sup>. The real and imaginary parts of the ac susceptibility,  $\chi'$  and  $\chi''$ , are presented in Figs. 1(b) and (d) (driving field 3.5 Oe). They show a frequency dependent peak in  $\chi'$  located slightly above a spin-freezing temperature  $T_{sf}$ , which is determined below. Figure 1(d) shows the temperature variation of this peak in  $\chi'$  with frequency. It was found that this could be fitted to the

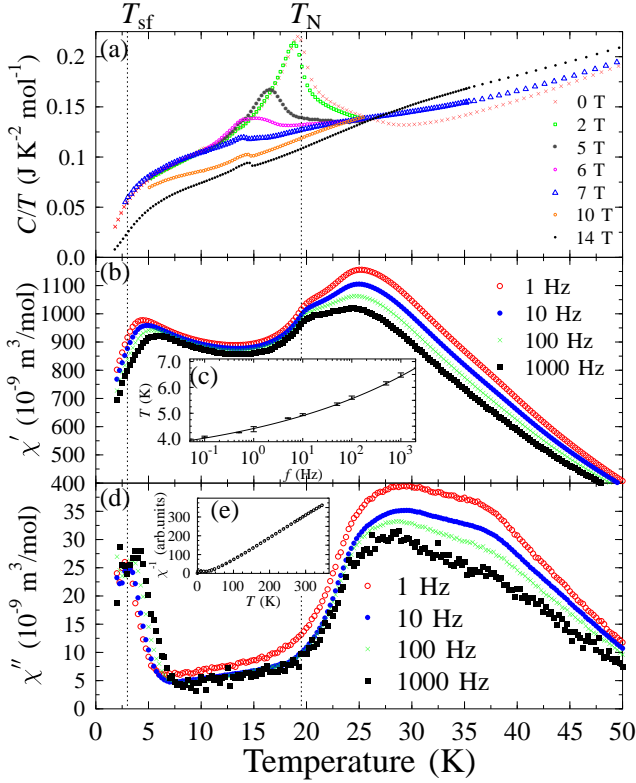


FIG. 1: (Color online) The panels correspond to: (a) Heat capacity divided by temperature in fields between 0 and 14 T. (b) Real part,  $\chi'$ , of the ac magnetic susceptibility. (c) Temperature dependence of the peak in  $\chi'$  associated with  $T_f$  with a fit to the Ogielski relation (Eq. (1)). (d) Imaginary part,  $\chi''$ , of the ac magnetic susceptibility. (e) Inverse of magnetic susceptibility data against temperature with a linear fit showing the high-temperature Curie-Weiss behavior. The vertical dashed lines indicate temperatures referred to in the text.

Ogielski scaling relation<sup>23</sup>:

$$T = T_{sf}(1 + (f\tau_0)^{1/z\nu_c}), \quad (1)$$

where  $T$  is the temperature of the peak in  $\chi'$ ,  $f$  is the measurement frequency,  $\tau_0$  is the relaxation time of the system,  $z$  is a dynamic exponent, and  $\nu_c$  is a critical exponent. Fitting the data to Eq. (1) gives  $T_{sf} = 3 \pm 0.2$  K,  $\tau_0 = 5.4(2) \times 10^{-3}$  s and  $z\nu_c = 8.1 \pm 0.4$ . This is typical of glassy behavior or the slowing of spin fluctuations. Given that muon precession was observed down to 1.6 K (see below), the formation of a true spin glass around  $T_{sf}$  is excluded. One possible interpretation of the feature around  $T_{sf}$  is that it could arise from a small concentration of defects comprised of pairs of  $\text{Ni}^{2+}$  impurity spins which are associated with oxygen vacancies. Alternatively, the fluctuations in the spins could be slowing down around  $T_{sf}$ . At  $T_N$ ,  $\chi'$  has a small maximum and rises to a larger peak near 25 K, with the frequency dependence increasing from  $T_N$  to the peak, and decreasing above it. The temperature of the peak in  $\chi'$  at 25 K decreases slowly with increasing frequency, which may

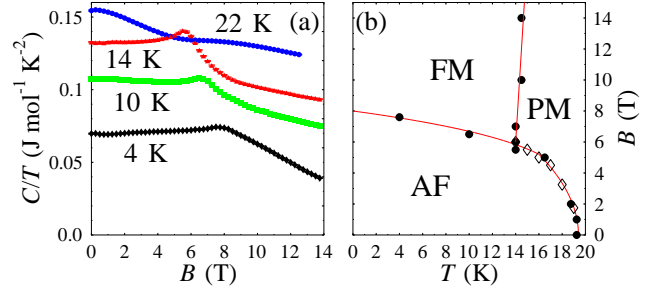


FIG. 2: (Color online) (a) Heat capacity divided by temperature vs field at four temperatures. (b) Partial magnetic phase diagram deduced from heat capacity ( $\bullet$ ) and magnetization ( $\diamond$ ) data. AF: A-type antiferromagnetic phase. PM: Paramagnetic phase. FM: Ferromagnetic phase.

be related to the presence of two sets of relaxation times varying differently with temperature (see below).  $\chi''$  also rises sharply near 25 K but to a plateau continuing up to  $\sim 35$  K. Together these suggest that short-range order persists up to  $\sim 25$  K, that slowly fluctuating clusters of spins are present within a fast fluctuating paramagnetic bulk above this temperature, and that the volume fraction of clusters decreases with increasing temperature.

Constant temperature heat capacity data with varying magnetic field are presented in Fig. 2(a). Except for the data taken at 22 K, a peak is observed which corresponds to the field labelled  $H_{C1}$  in the magnetization data reported in Ref. 16. This suggests that this marks the upper field boundary of A-type antiferromagnetic order. At 22 K the heat capacity decreases with increasing field consistent with short-range order. The partial magnetic phase diagram deduced from our heat capacity and magnetization data is shown in Fig. 2(b).

Our zero-field  $\mu$ SR experiments were carried out using the DOLLY instrument at the Paul Scherrer Institute (PSI), Villigen, Switzerland. In our  $\mu$ SR experiments, spin polarized positive muons ( $\mu^+$ , mean lifetime 2.2  $\mu$ s, momentum 28 MeV/c) were implanted into polycrystalline  $\text{NaNiO}_2$ . The decay positron asymmetry function,  $A(t)$ <sup>22</sup>, is proportional to the average spin polarization of the muons stopped within the sample. The muon spin precesses around an internal magnetic field,  $B_\mu$ , at a frequency  $\nu_\mu = (\gamma_\mu/2\pi)|B_\mu|$ , where  $\gamma_\mu/2\pi = 135.5$  MHz  $\text{T}^{-1}$ .

The asymmetry data were fitted to Eq. (2)<sup>24</sup> below  $T_N$ , and to Eq. (3) above  $T_N$ :

$$A(t) = A(0) (P_1 e^{-\lambda_1 t} + P_2 e^{-\lambda_2 t} \cos(2\pi\nu_\mu t + \phi_0)) \quad (2)$$

$$A(t) = A(0) (P_f e^{-\lambda_f t} + P_s e^{-\lambda_s t}), \quad (3)$$

where  $A(0)$  is the initial asymmetry.  $P_1$  and  $P_2$  are respectively the longitudinal and transverse components of the muon polarization, and  $P_1 + P_2 = 1$ . The exponential relaxation associated with  $P_1$  reflects the dynamical fluctuations of the fields being probed. The  $P_2$  term describes muon precession with a distribution of local fields

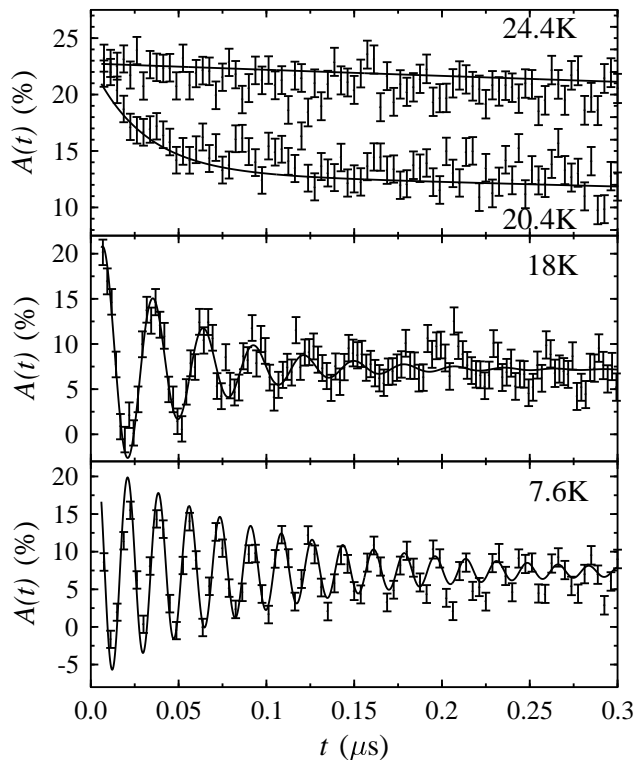


FIG. 3: Muon decay asymmetry in  $\text{NaNiO}_2$  plotted at different temperatures. The solid lines are fits of the data to Eqs. (2) & (3) with the parameters shown in Fig. 4.

dephasing the muon spins. In a fully magnetically ordered polycrystalline sample we expect  $P_2/P_1 = 2$ . Coherent muon precession will be observed if long range order is present within the sample.  $P_s$  and  $P_f$  describe slow and fast dynamic fluctuations respectively. A small initial phase offset,  $\phi_0$ , was observed below  $T_N$ , larger than could be attributed to errors in determining the time that the muons enter the sample. This could be produced by a small magnetic inequivalency in the position of muons stopped within the sample, consistent with an asymmetric peak seen in Fourier transforms of the data. In the fitting procedure, data were fitted in the time range  $0 < t < 8 \mu\text{s}$ , where the effect of background counts could be reliably subtracted. Rapid dynamic fluctuations lead to  $\lambda_1 \propto \gamma_\mu^2 (\Delta B)^2 / \nu$ , where  $\Delta B$  is the amplitude of the fluctuating local field and  $\nu$  is the fluctuation rate<sup>24</sup>.

Spectra measured at four temperatures are shown in Fig. 3. There are three distinct temperature regions apparent from the muon asymmetry spectra. At low temperatures ( $T \leq 19.5 \text{ K}$ ) there are clear oscillations in the asymmetry showing that long range magnetic order exists and the observed ratio of  $P_2 : P_1 \approx 2$  (see Fig. 4(b)) indicates that the sample is magnetic over its entire volume. The value of  $\lambda_{2,s}$  is much larger than  $\lambda_{1,f}$  (see Fig. 4(c) & (d)) so at short times only the effect of  $\lambda_{2,s}$  is seen in Fig. 3. An intermediate temperature range ( $19.5 < T < 24 \text{ K}$ ) gives no oscillations, and the relax-

ation is modelled with the two exponential components of Eq. (3), with the amplitude of the faster relaxing component decreasing with increasing temperature. Above 24 K the relaxation is well described by a single exponential,  $P_f \exp(-\lambda_f t)$ , consistent with fast fluctuations of paramagnetic moments characterized by a single correlation time in the muon time window.

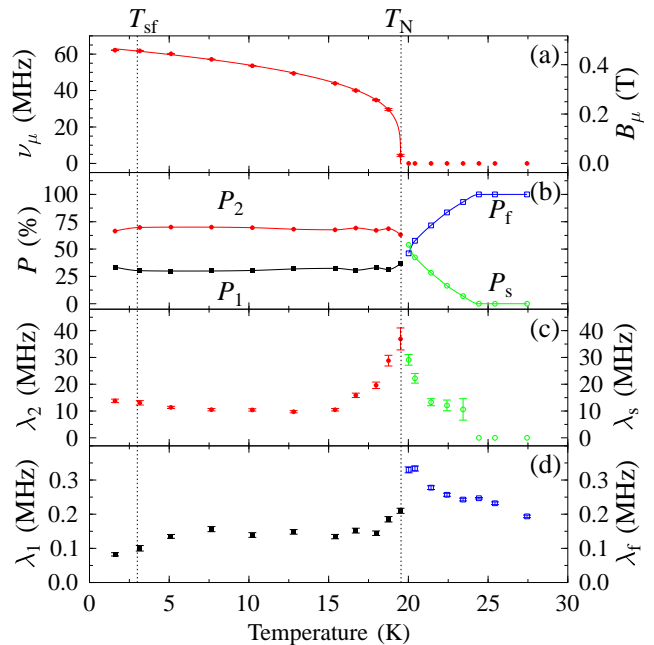


FIG. 4: (Color online) Temperature dependence of the parameters determined from fitting data to Eqs. (2) & (3): (a) the oscillation frequency,  $\nu_\mu$ , and the internal magnetic field,  $B_\mu$ , with a fit to Eq. (4). (b) Amplitudes of the relaxation components  $P_1$  and  $P_2$ , and  $P_f$  and  $P_s$ . (c) Relaxation rates  $\lambda_2$  and  $\lambda_s$ . (d) Relaxation rates  $\lambda_1$  and  $\lambda_f$ . The vertical dashed lines indicate temperatures referred to in the text.

The temperature dependence of the parameters derived from fitting Eqs. (2) & (3) to muon asymmetry spectra are presented in Fig. 4. The muon precession frequency,  $\nu_\mu$ , in the ordered phase is shown in Fig. 4(a). This is proportional to the sublattice magnetization at the muon site, and was fitted to a function<sup>25</sup>:

$$\nu_\mu(T) = \nu_\mu(0)(1 - (T/T_N))^{\beta_m}. \quad (4)$$

The fit gives  $\nu_\mu(0) = 64.2(2) \text{ MHz}$  corresponding to a field at the muon site of  $\sim 0.5 \text{ T}$ . Dipole field calculations show that this field will be experienced by muons near any of the oxygen atoms in the octahedron surrounding a nickel atom, in regions of high electron density<sup>26</sup>, and show that our results are consistent with the magnetic structure determined by Darie et al.<sup>11</sup>. Our calculations also suggest that the muon precession frequency is insensitive to small deviations from this magnetic structure. Fitting Eq. (4) to the muon precession frequencies gave  $T_N = 19.51(1) \text{ K}$  and  $\beta_m = 0.24(1)$ . This value of  $\beta_m$  suggests that the system is behaving as a 2D XY magnet<sup>27</sup>.

In relation to the peak just above  $T_{sf}$  in the magnetic susceptibility, we note that extrapolating the Ogielski scaling relation to the muon time window suggests a maximum in the dynamic relaxation rate  $\lambda_1$  should be observed around 7 K, and a broad maximum of low amplitude is just detectable at this temperature (Fig. 4(d)). The presence of two exponential relaxation components above  $T_N$  (see Eq. (3)) suggests that short-range magnetic order persists over a small temperature range of  $\sim 5$  K above  $T_N$ . The fluctuations in the magnetic field producing the faster relaxing component,  $\lambda_s$ , are two orders of magnitude slower than those producing the slowly relaxing component,  $\lambda_f$ .  $P_s$  decreases with increasing temperature up to 24 K, showing that the ratio of slow to fast dynamic relaxation is decreasing. Above this temperature the muon relaxation is that expected for a system in the fast-fluctuation regime. The slow spin relaxations observed in the frequency dependence of the ac susceptibility above 25 K are not within the muon time window so are not observed. The observation of two components in the muon relaxation below 24 K, together with a changing frequency dependence of the ac susceptibility, suggest a model of coalescing magnetic clusters forming well above  $T_N$ . On cooling below  $\sim 50$  K, these magnetic clusters occupy an increasing volume fraction, causing the increase in the frequency dependence of the ac susceptibility, until at  $\sim 25$  K the sample possesses

short-range antiferromagnetic order. Below 25 K these clusters coalesce, leading to the decrease in the frequency dependence of the ac susceptibility, and the increase in  $P_s$ , until at  $T_N$  the sample possesses long-range order. Short-range order within the layers and antiferromagnetically correlated layers is consistent with the persistence of unbroadened magnetic Bragg peaks observed by neutron powder diffraction over a similar temperature range above  $T_N$ <sup>12,28</sup>.

In conclusion,  $\text{NaNiO}_2$  shows the onset of long-range magnetic order at  $T_N = 19.5$  K, with the dependence of the sublattice magnetization on temperature appropriate for a 2D XY magnet. The slowing of spin fluctuations above  $T_{sf}$  is evident in the ac magnetic susceptibility data. At temperatures just above  $T_N$  there is evidence of short-range order, and of magnetic clusters persisting within a paramagnetic phase above this temperature.

Part of this work was performed at the Swiss Muon Source, Paul Scherrer Institute, Villigen, Switzerland. We are grateful to Robert Scheuermann for experimental assistance, and to M. Holzapfel, B. D. Gaulin, and A. Coldea for helpful discussions. T. L. acknowledges support from the European Commission under the 6<sup>th</sup> Framework Programme through the Key Action: Strengthening the European Research Area, Research Infrastructures. Contract no: RII3-CT2003-505925. This work was funded by the EPSRC (UK).

- 
- <sup>1</sup> J. S. Gardner, B. D. Gaulin, S.-H. Lee, C. Broholm, N. P. Raju, and J. E. Greedan, *Phys. Rev. Lett.* **83**, 211 (1999).  
<sup>2</sup> F. Mila, *Eur. J. Phys.* **21**, 499 (2000).  
<sup>3</sup> J. Snyder, J. S. Slusky, R. J. Cava, and P. Schiffer, *Nature* **413**, 48 (2001).  
<sup>4</sup> M. F. Collins and O. A. Petrenko, *Can. J. Phys.* **75**, 605 (1997).  
<sup>5</sup> R. Coldea, D. A. Tennant, and Z. Tylczynski, *Phys. Rev. B.* **68**, 134424 (2003).  
<sup>6</sup> S. Kobayashi, S. Mitsuda, M. Ishikawa, K. Miyatani, and K. Kohn, *Phys. Rev. B.* **60**, 3331 (1999).  
<sup>7</sup> B. C. Sales, R. Jin, K. A. Affholter, P. Khalifah, G. M. Veith, and D. Mandrus, *Phys. Rev. B.* **70**, 174419 (2004).  
<sup>8</sup> T. Chatterji, W. Henggeler, and C. Delmas, *J. Phys. Condens. Matter* **17**, 1341 (2005).  
<sup>9</sup> H. Kikuchi, H. Nagasawa, M. Mekata, Y. Fudamoto, K. M. Kojima, G. M. Luke, Y. J. Uemura, H. Mamiya, and T. Naka, *Hyperfine Interact.* **120-121**, 623 (1999).  
<sup>10</sup> M. D. Núñez-Regueiro, E. Chappel, G. Chouteau, and C. Delmas, *Eur. Phys. J. B.* **16**, 37 (2000).  
<sup>11</sup> C. Darie, P. Bordet, S. de Brion, M. Holzapfel, O. Isnard, A. Lecchi, J. E. Lorenzo, and E. Suard, *Eur. Phys. J. B.* **43**, 159 (2005).  
<sup>12</sup> M. J. Lewis, B. D. Gaulin, L. Filion, C. Kallin, A. J. Berlinsky, H. A. Dabkowska, Y. Qiu, and J. R. D. Copley, (unpublished), cond-mat/0409727.  
<sup>13</sup> P. F. Bongers and U. Enz, *Solid State Commun.* **4**, 153 (1966).  
<sup>14</sup> J. P. Kemp, P. A. Cox, and J. W. Hodby, *J. Phys. Condens. Matter* **2**, 6699 (1990).  
<sup>15</sup> E. Chappel, M. D. Núñez-Regueiro, F. Dupont, G. Chouteau, C. Darie, and A. Sulpice, *Eur. Phys. J. B.* **17**, 609 (2000).  
<sup>16</sup> M. Holzapfel, S. de Brion, C. Darie, P. Bordet, E. Chappel, G. Chouteau, P. Strobel, A. Sulpice, and M. D. Núñez-Regueiro, *Phys. Rev. B.* **70**, 132410 (2004).  
<sup>17</sup> E. Chappel, M. D. Núñez-Regueiro, G. Chouteau, O. Isnard, and C. Darie, *Eur. Phys. J. B.* **17**, 615 (2000).  
<sup>18</sup> S. Tornow, O. Entin-Wohlman, and A. Aharony, *Phys. Rev. B.* **60**, 10206 (1999).  
<sup>19</sup> A.-M. Daré, R. Hayn, and J.-L. Richard, *Europhys. Lett.* **61**, 803 (2003).  
<sup>20</sup> F. Vernay, K. Penc, P. Fazekas, and F. Mila, *Phys. Rev. B.* **70**, 014428 (2004).  
<sup>21</sup> A. J. W. Reitsma, L. F. Feiner, and A. M. Oleś, *New J. Phys.* **7**, 121 (2005).  
<sup>22</sup> S. J. Blundell, *Contemp. Phys.* **40**, 175 (1999).  
<sup>23</sup> A. T. Ogielski, *Phys. Rev. B.* **32**, 7384 (1985).  
<sup>24</sup> P. Dalmas de Réotier and A. Yaouanc, *J. Phys. Condens. Matter* **9**, 9113 (1997).  
<sup>25</sup> F. Borsa, P. Carreta, J. H. Cho, F. C. Chou, Q. Hu, D. C. Johnston, A. Lascialfari, D. R. Torgeson, R. J. Gooding, N. M. Salem, et al., *Phys. Rev. B.* **52**, 7334 (1995).  
<sup>26</sup> H. Meskine and S. Satpathy, *J. Appl. Phys.* **97**, 10A314 (2005).  
<sup>27</sup> S. T. Bramwell, P. C. W. Holdsworth, and M. T. Hutchings, *J. Phys. Soc. Jpn.* **64**, 3066 (1995).  
<sup>28</sup> B. D. Gaulin, (private communication).